Mississippi State University
Scholars Junction

Theses and Dissertations | Theses and Dissertations

1-1-2011

Spectroscopic Investigations of 2,4,6-Trinitrotoluene (TNT)

Tracy Stevens Miller

Follow this and additional works at: https://scholarsjunction.msstate.edu/td

Recommended Citation

Miller, Tracy Stevens, "Spectroscopic Investigations of 2,4,6-Trinitrotoluene (TNT)" (2011). *Theses and Dissertations*. 4027.
https://scholarsjunction.msstate.edu/td/4027

This Graduate Thesis - Open Access is brought to you for free and open access by the Theses and Dissertations at Scholars Junction. It has been accepted for inclusion in Theses and Dissertations by an authorized administrator of Scholars Junction. For more information, please contact scholcomm@msstate.libanswers.com.

SPECTROSCOPIC INVESTIGATIONS OF 2,4,6-TRINITROTOLUENE (TNT)

By

Tracy Stevens Miller

A Thesis
Submitted to the Faculty of
Mississippi State University
in Partial Fulfillment of the Requirements
for the Degree of Master of Science
in Physics
in the Department of Physics and Astronomy

Mississippi State, Mississippi

August 2011

SPECTROSCOPIC INVESTIGATIONS OF 2,4,6-TRINITROTOLUENE (TNT)

By

Tracy Stevens Miller

Approved:

David L. Monts Professor of Physics Major Professor Committee Member	Jagdish P. Singh Professor of Physics Major Professor Committee Member
Chun Fu Su Professor of Physics Committee Member	Mark Novotny Department Head and Professor Graduate Coordinator
Gary L. Myers Dean of the College of Arts and Sciences	

Name: Tracy Stevens Miller

Date of Degree: August 6, 2011

Institution: Mississippi State University

Major Field: Physics

Major Professor: Dr. David Monts

Title of Study: SPECTROSCOPIC INVESTIGATIONS OF 2,4,6-TRINITROTOLUENE (TNT)

Pages in Study: 55

Candidate for Degree of Master of Science

Spectroscopic studies using absorption spectroscopy (AS), photofragmentation spectroscopy (PF-LIF), and cavity ringdown spectroscopy (CRDS) were preformed on 2,4,6-Trinitrotoluene. The NO detection of the energetic material (EM) was done using combinations of the previous procedures. Calculations for the absorption coefficient and cross sections were obtained. The procedure of photofragmentation required heating of the sample to generate an absorption curve and a cross section. Absorption spectroscopy, which covered a range of 195-300 nm, also corresponded with the use of heating the sample to obtain the two values. Cavity ringdown spectroscopy investigations were done on the sample at room temperature. A higher accuracy for the level of detection was obtained using a combination of photofragmentation at various wavelengths and cavity ringdown spectroscopies.

ACKNOWLEDGEMENTS

.I am grateful to God for allowing this work to take place. Appreciation and admiration go to Dr. Monts, Dr. Singh, Dr. Su, and Fang Yu Yueh for the mentorship and patience placed upon me in the understanding of the subject of my thesis.

Special gratitude is to be given to Dr. Monts, Dr. Singh, and Fang Yu Yueh for the input and for the instruction of making this thesis possible. Special consideration is to be given to Dr. Mark A. Novotny for the duration of the program.

Consideration is to be given to the ICET family from the shop to the administrative staff in the assistance outside of the laboratory.

Last but not least, I thank my families for the support, encouragement, and belief of me completion the program.

We finally did it.

TABLE OF CONTENTS

LIST OF TABLES

LIST OF FIGURES

CHAPTER I

INTRODUCTION

The National Priorities List as well as the EPA (Environmental Protection Agency) have given several characteristics of compounds which would classify as human carcinogens. Many energetic materials (EMs) such as TNT (2,4,6-Trinitrotoluene) fall into these categories. The long-term effects of energetic materials have become major concerns on their effects in the environment, not only near military sites but in surrounding areas populated as well as non-populated. Drinking water, air in the environment, food chains, and soil are possible transmissions of these containments making them useless. Methods of detection and extraction have been used:

1. GC/MS (gas chromatography-mass spectroscopy)
2. Photofragmentation Laser-induced Fluorescence (PF-LIF)
3. Absorption spectroscopy (AS)
4. Cavity ringdown spectroscopy.

The technique gas chromatography-mass spectroscopy requires the collection of data to be analyzed at a later time. This time frame can require hours which would have no value in data analysis needed in a short period.

Photofragmentation has been used over the years in the study of detection for NO in the UV region of TNT. A laser beam strikes the TNT which breaks it down to a molecule and NO_2. NO_2 is broken into oxygen and NO which fluoresces at 226nm. . Low levels of detection as low as 40 ppb have been found on TNT. On a sample,

photofragmentation and predissociation can occur at the same wavelength. A shortcoming of photofragmentation is requiring heat on the sample for better intensity. As heat is applied the intensity of the signal diminishes.

Absorption spectroscopy has a good detection if there is an abundance of the sample. As a light source is used upon the TNT sample, initial and final intensities are compared in the calculation of the absorbance coefficient of TNT. The absorbance coefficient has a dependence of the wavelength. Absorbance spectroscopy requires heat upon the sample as well.

Cavity ringdown spectroscopy can be used on TNT at room temperature rather an application of heat. Higher reflectivity of mirrors used in this technique give better levels of detection if the mirrors are designed for the region of interest. For the study done on TNT the wavelength was 226 nm. A better signal is obtained if the cell is lengthened also.

The use of these procedures was the analysis of TNT in the gaseous phase which has never been done before.

Levels of detections on TNT were compared using photofragmentation, cavity ringdown, and combinations of them.

The layout of my thesis is as follows: Chapter 1 gives fundamentals of spectroscopy, techniques of spectroscopy (photofragmentation laser-induced fluorescence, absorption), and the concepts of lasers. Also it gives properties of 2,4,6-trinitroluene. Chapter 2 covers experimentation and results of absorption spectroscopy combined with cavity ringdown spectroscopy in the UV region towards the calculation of the cross section and absorption coefficient of TNT. This was done in gaseous phase. Chapter 3 covers the optical properties of TNT in the gaseous ultraviolet regions.

Chapter 4 covers the photofragmentation cross sections of gaseous TNT at different wavelengths. An experimental combination of photofragmentation and cavity ringdown using filters of 254 nm, 300 nm, 340 nm, and 400 nm were used. An inverse relationship was found between the cross sections and the wavelengths of TNT. Procedures were performed on gaseous TNT in the calculation of the cross section. Combinations of techniques gave better results on levels of detection rather than each being performed individually. Chapter 5 gives the summary.

CHAPTER II

FUNDAMENTALS OF SPECTROSCOPY

Types of Energy

There are three main types of energy levels studied by molecular spectroscopy: rotational, vibrational, and electronic[1]. A summation of these energies gives the total energy:

$$E = E_r + E_v + E_e \tag{2.1}$$

where the subscripts represent the types of energies - rotational, vibrational, and electronic.

A similar feature takes place with the wave functions:

$$\psi = \psi_r * \psi_v * \psi_e . \tag{2.2}$$

According to the Born-Oppenheimer approximation, the electronic and nuclear motions of a molecule can be separated because the motion of the nuclei is slow compared to the motion of electrons. A larger number of motions occur in a polyatomic molecule than in a diatomic molecule. The number of vibrational normal modes in a polyatomic molecule is 3N-6 (3N-5 if the molecule is linear) where N is the number of atoms in the molecule [2]. The vibrational normal modes can be assigned and analyzed classically and quantum mechanically. There is a similarity between vibrational motion and the harmonic oscillator. Motion of a diatomic molecule is comparable to a particle of reduced mass μ in a centrally symmetric field; however this simplified approach is not

possible when dealing with polyatomic molecules, although the harmonic oscillator energy is still valid.

Vibrational and rotational motions are complicated, even from a classical standpoint. The more complicated the molecular structure of an analyte, the more complicated is its spectrum. Rotational energies are typically less than vibrational energies. If vibrational motion is excited, so also will rotational motion become excited. When excited, a molecule goes to a state of higher energy and the rotational energy and/or vibrational energy increases. In generating spectra from the vibrational, rotational, and electronic energy levels, interest lies only in the ones that change. For example, in studying a rotational spectrum, there is a change in rotational energy with the electronic and vibrational energies remaining constant. In generating a rotation-vibration spectrum, there is a change in the rotational level of a given vibrational level to a rotational level of another vibrational level while the electronic state remains the same. When recording an electronic spectrum, there is a change in the rotational level of various vibrational levels of one electronic state to rotational and vibrational levels of another electronic state; such transitions are referred to as "ro-vibronic" (rotational-vibrational-electronic).

The easiest model for the rotational levels of a diatomic molecule is the dumbbell where two masses are separated by a distance r[1]. The energy of rotation is

$$E_r = \frac{I_r \omega^2}{2} \tag{2.3}$$

where the value of I_r denotes the inertia perpendicular to the line between m_1 and m_2, and ω is the angular frequency. From a polyatomic standpoint, the inertia can be written as a summation of the inertia:

$$I_r = \frac{1}{2M} m_i m_j r_{ij}^{\ 2} \tag{2.4}$$

where M is the total mass of m_i and m_j separated by distance r_{ij}. Using Cartesian coordinates,

$$\begin{aligned} I_x &= \sum_i m_i (y_i^{\ 2} + z_i^{\ 2}) & I_{xy} &= \sum_i m_i x_i y_i \\ I_y &= \sum_i m_i (x_i^{\ 2} + z_i^{\ 2}) & I_{yz} &= \sum_i m_i y_i z_i \\ I_z &= \sum_i m_i (x_i^{\ 2} + y_i^{\ 2}) & I_{xz} &= \sum_i m_i x_i z_i \\ & & I_{xy} &= I_{yx} \end{aligned} \tag{2.5}$$

where

$$I_x x^2 + I_y y^2 + I_z z^2 - 2I_{xy} xy - 2I_{yz} yz - 2I_{zx} zx = 1. \tag{2.6}$$

The representation of the momentum ellipsoid is a quadric surface.

The angular momentum (P) is the product of the inertia and the angular frequency:

$$P = I\omega \tag{2.7}$$

Only certain rotational energy levels can satisfy the Schrödinger equation. The energy is calculated by the momentum squared divided by twice the inertia

$$E_r = \frac{P^2}{2I} \tag{2.8}$$

Other variables are also used in dealing with rotation. The energy of rotation can also be written as:

$$E_r = \frac{h^2 J(J+1)}{8\pi^2 \mu r^2} = \frac{h^2 J(J+1)}{8\pi^2 I}. \tag{2.9}$$

The values of J represent the discrete rotational quantum number and are non-negative integers (0, 1, 2, …). The variable h is Planck's constant (6.62×10^{-34} J·s), and μ is the reduced mass

$$\mu = \frac{m_1 m_2}{m_1 + m_2} \quad (2.10)$$

The selection rules for rotational energy correspond to J→J or J→J±1; J→J±2 transitions are forbidden or weak for electric dipole-allowed transitions. A change in energy is a function of the rotational quantum number; for example, for a J→J+1 transition, the change in the rotational energy is:

$$\Delta E = B(J+1)(J+2) - BJ(J+1) = 2B \quad (2.11)$$

Where B is the rotational constant in cm^{-1} and is defined below. The absolute value of the momentum can be calculated as the square root of the numerator of the rotational energy, Eqn 1.9. Also the rotational term energy, F(J), is defined by:

$$F(J) = \frac{E_r}{hc} = BJ(J+1). \quad (2.12)$$

In this equation, B represents the rotational constant,

$$B = \frac{h}{8\pi^2 cI} = \frac{h}{8\pi^2 c\mu r^2} \quad (2.13)$$

where c is the speed of light in a vacuum (2.99×10^8 m/s) and r represents the internuclear distance of a diatomic molecule. This value is inversely proportional to the inertia. The rotational eigenfunctions of the time-independent Schrödinger equation are the spherical harmonics based on the values of the rotational quantum number J. A value referred to as the magnetic quantum number, M_j, is also based on the value of J, and it ranges from the absolute J to -J. (The number of M_j values present is 2J+1). A product of the

magnetic quantum and ħ (Planck's constant h divided by 2 π) is the component of the angular momentum J in the z-direction. If the molecule is not rigid, the rotational value requires introduction of a correction term, the centrifugal distortion constant D:

$$F(J) = BJ(J+1) - DJ^2(J+1)^2 \tag{2.14}$$

$$D \approx \frac{4B^3}{\omega^2}, \tag{2.15}$$

where ω in the vibrational angular frequency (in cm^{-1}), which differs from the normal vibrational frequency ν by a factor of 2π.

A good representation of vibrational motion of a diatomic molecule is the harmonic oscillator. The potential energy is half the product of the force constant k and the square of the displacement. The spatial difference ($r-r_e$) is the change of the instantaneous internuclear distance r from the equilibrium internuclear distance r_e. This is the same as the displacement of the oscillator x from the equilibrium point:

$$V = \tfrac{1}{2}kx^2 = \tfrac{1}{2}k(r-r_e)^2 \tag{2.16}$$

Stronger bonds have larger force constants k.

In terms of the reduced mass, the force constant (k) is written as

$$k=4\mu\pi^2\nu_{osc}{}^2 \tag{2.18}$$

where ν_{osc} , the oscillation frequency, is measured in cm^{-1} and μ is the reduced mass as mentioned for rotational energy. The energy for the harmonic oscillator is calculated by

$$E = h\nu_{osc}(\mathrm{v}+\frac{1}{2}) \tag{2.19}$$

where v= 0, 1, 2,… and is the vibrational quantum number. The vibrational term energy, G(v), is approximately represented by:

$$G(\mathrm{v}) = \frac{E_v}{hc} = \omega(\mathrm{v} + \frac{1}{2}) \tag{2.20}$$

Here the angular frequency ω is of the form

$$\omega = \frac{\upsilon_{osc}}{2\pi} \tag{2.21}$$

The vibrational eigenfunctions of a harmonic oscillator are Hermite orthonormal functions. The lowest level of energy in the vibrational spectrum (v=0) is non-zero; it has energy of ½ħω. This wave function is Gaussian. In actuality, the molecule is not firmly a harmonic oscillator, but an anharmonic oscillator; the potential function mentioned above is not perfectly parabolic in nature, but can be rewritten with additional cubic and higher-power terms.

The Morse function is a commonly used electronic molecular potential of the the form

$$V = D_e[1 - e^{-\beta(r-r_e)}]^2 \tag{2.22}$$

where D_e is the dissociation energy or energy difference between asymptote and minimum potential E;

$$\beta = \sqrt{\frac{2\pi^2 c\mu}{D_e h}}\omega_e = 1.21\bar{7}x10^7\,\omega_e\sqrt{\frac{\mu_A}{D_e}} \tag{2.23}$$

and μ_A is the reduced mass in atomic units.

In finding the value of vibrational energy for an anharmonic oscillator, G(v) is rewritten with additional terms obtained by substituting into the wave equation:

$$G(\mathrm{v}) = \omega_e(\mathrm{v} + \tfrac{1}{2}) - \omega_e x_e(\mathrm{v} + \tfrac{1}{2})^2 + \omega_e y_e(\mathrm{v} + \tfrac{1}{2})^3 + \cdots \tag{2.24}$$

where the products of frequency and distance are quite small compared to frequency alone: $\omega_e x_e << \omega_e$ and $\omega_e y_e << \omega_e{}^2$. The zero state of energy is the minimum of G(v).

Relative to the lowest level (v=0), G(v) is rewritten as

$$G_0(\mathrm{v}) = \omega_0 \mathrm{v} - \omega_0 x_0 \mathrm{v}^2 + \omega_0 y_0 \mathrm{v}^3 + \cdots \tag{2.25}$$

As mentioned above, the relationship between the frequency and spatial components still holds. The spacing between successive vibrational energy levels is not constant, but rather it decreases to zero as the dissociation limit is approached. The number of levels here is finite; in the case of a Coulomb potential, the number of vibrational levels is infinite. Separation between successive levels of vibration is given by

$$\Delta G(\mathrm{v}+\tfrac{1}{2}) = G(\mathrm{v}+1) - G(\mathrm{v}) \tag{2.26}$$

Substitution back into the aforementioned equation for the vibrational energy, the separation between successive levels is written as:

$$\Delta G(\mathrm{v}+\tfrac{1}{2}) = (\omega_e - \omega_e x_e + \omega_e y_e + \cdots) - (2\omega_e x_e - 3\omega_e y_e - \cdots)(\mathrm{v}+\tfrac{1}{2}) + 3\omega_e y_e (\mathrm{v}+\tfrac{1}{2})^2 + \cdots \tag{2.27}$$

As the frequency increases the energy separation decreases.

In a molecule, rotation and vibration occur simultaneously and must interact. If vibrational motion occurs, the internuclear distance must change, changing the moment of inertia. Because of this, the rotational constant B (rewritten as a function of frequency) for a given vibrational level v differs from the rotational constant for the equilibrium position, B_e. The spatial dependence in the rotational constant is now an average over the changing internuclear distances:

$$B_\upsilon = \frac{h}{8\pi^2 c\mu}\frac{1}{r_{avg}{}^2} \tag{2.28}$$

In terms of the rotation constant of the equilibrium position, B_e, the rotational constant as a function of vibrational quantum number is written as

$$B_\upsilon = B_e - \alpha_e(\upsilon + \tfrac{1}{2}) + \cdots \tag{2.29}$$

where α_e, the vibration-rotation interaction constant, is a function of the anharmonicity of the vibration. The subscript e in the above equation represents equilibrium. The rotational constant for equilibrium only changes in terms of the distance compared to B above:

$$B_e = \frac{h}{8\pi^2 c\mu r_e{}^2} \tag{2.30}$$

Another rotational constant called the centrifugal distortion constant, D_v gives an expression of the centrifugal force of and is written as

$$D_v = D_e + \beta_e(v + \tfrac{1}{2}) + \ldots \tag{2.31}$$

where D_e is value of the centrifugal distortion constant at equilibrium and β_e is a correction term as is α_e in the previous equation. It is shown that both of the previous equations are dependent on the magnitude of the vibrational motion and on the value of the vibrational quantum number v.

Pertaining to electronic states, a good example given by Herzberg[1] is an electronic state in the presence of two fixed nuclei. To further elaborate, Herzberg uses the H_2^+ ion. In solving the time-independent Schrödinger equation for this particular setup, discreteness (quantization) only comes into being when the energy is negative; any energy value is possible when it is positive. Certain negative energy values can be obtained from "united atoms" by application of a strong electric field. In the united-atom

method, the nuclei are assumed to be so close that the electronic states build up as they do in the atomic case. In the separated-atom method, the electron distribution of each atom is considered independently initially; then the two are put together. The asymptotic limit for the molecule at large internuclear separations approaching dissociation is covered by this method. The principal quantum number, n, and the azimuthal or orbital angular momentum quantum number, *l*, are used in the united-atom method. The orbital quantum number is written in units of ħ. The vector $\vec{l}$ represents the electronic orbital angular momentum, and is related to the electronic angular momentum operator l^2 and also λthe orbital angular momentum quantum number *l*. The eigenvalues of l^2:

$$\vec{l} = \sqrt{l(l+1)}\,\frac{h}{2\pi} \approx l\hbar \tag{2.32}$$

If an electric external field exists, the vector can only be orientated with regard to the field direction for which its component in the field direction is equivalent to

$$\frac{m_l h}{2\pi} \tag{2.33}$$

where $m_l = l, l-1, l-2, \cdots, -l$.

Syntax of Spectroscopy

Orbitals (orbital wave functions) of one-electron states where the *l* quantum number has the value of 0,1,2,… are called σ, π, δ,… orbitals whereas molecular electrons in these are called σ,π,δ,… ; this is similar to where the letters s, p, d,… which represent atomic electrons (orbitals) with angular momentum quantum numbers *l*= 0,1,2,… respectively. The number of electrons per shell is given $2(2l+1)$. When *l* =0, two electrons may be are in, the s shell; when *l* is 1, six electrons can be present, in the p shell*, etc.*[2]. Orbitals with *l*≠0 have two values since $m_j = \pm l$ and are referred to as being

doubly degenerate Orbitals with l=0 have only one function and are called nondegenerate. A situation called lambda-doubling is introduced in the coupling of electronic and rotational modes where $l \neq 0$.

Identification of atomic electrons is of the format of n, l, m_j. The n and l values of a united atom are used to set apart different σ, π, δ,… orbitals[1]. These are written as 1sσ, 2sσ, 2pσ, 2pπ, 3sσ, 3pσ, 3pπ, 3dσ, 3dπ, 3dδ, etc. The number given represents the value of n and s, p, d, … represent the l value of the united atom. In the case of the separated atom concept, a subscript is attached to the l value to denote which atom in a heteronuclear diatomic molecule, $\sigma 1s_H, \pi 2p_o, etc$. If two atoms are the same in a separated atom scheme (homonuclear diatomic molecule), they are given a subscript of g or u, such as $\sigma_g 1s$ or $\pi_u 2p$, where the g and the u stand for the German gerade (even) or ungerade (odd) parity. A homonuclear diatomic molecule is one which is made of one element. In the united case, if l is even, the 2nd orbital is even (g), the wave is considered symmetric; if l is odd, the 2nd orbital is odd (u), the wave is not symmetric. Symmetry plays an important role in selection rules.

Multi-Electron Systems

In a multi-electron system the quantum numbers n and l (each subscripted i) are used to distinguish each electron from the other. Each molecular state of a diatomic molecule will be identified by a total electronic orbital angular momentum quantum number

$$\vec{\Lambda} = \sum_i \vec{\lambda}_i \tag{2.34}$$

The vector notation accounts for the direction of $\vec{\lambda}_i$, all of which are aligned relative to the internuclear molecular axis. When Λ=0, 1, 2, 3,…, these states are referred

to as Σ, Π, Δ, Φ,… states respectively. Each of these with the exception of Σ is doubly degenerate (Λ>0) due to the opposite directions $\vec{\Lambda}$ can point. There are also components of various angular momentum vectors along the internuclear axis. The state formed is determined by the electron spin multiplicity of 2S+1 which is formed from the resultant total electron spin angular momentum $\vec{S}$. This spin is a summation of the individual valence electron spins $\vec{s}_i$:

$$\vec{S} = \sum_i \vec{s}_i . \tag{2.35}$$

If a molecule is homonuclear, it is assigned a subscript g or u depending on whether the parity of the orbitals is odd (u) or even (g).

The states of their wave functions are either symmetric or antisymmetric on reflection about any plane through the internuclear axis. States that are symmetric are assigned the superscript of + while those that are antisymmetric are assigned the superscript of ---. The electron spin multiplicity of each state is indicated by a preceding superscript ($^1\Sigma^+$, $^1\Sigma^-$, etc.). Equivalent valence electrons have the same values for *n* and *l*; when this is so, the Pauli exclusion principle requires that no two electrons in a particle possess the same quantum numbers n, *l*, m_l, m_s. No more than two electrons can exist in a given σ orbital; this can only come about if they have antiparallel spins. Larger orbitals (π, δ,…) can have a maximum of four electrons since m_l=±l and m_s=±½. The outer shell of the atom or molecule determines the electronic state of the atom or molecule observed.

Beer's Law

The attractiveness of absorption spectroscopy includes the ability of recording and analyzing spectra. The Beer-Lambert law is a linear relationship between absorbance A and concentration of an absorbing species. It is written as

$$A=\varepsilon Cl \tag{2.36}$$

where A is absorbance (dimension less), ε is the extinction coefficient ($mole^{-1}cm^{-1}$), C is concentration of sample (mole/liter), and l is length (cm). ε is also called molar absorptivity and is a function of wavelength. The variable ε(λ) tells how strongly a substance absorbs light at wavelength λ.

In terms of intensity,

$$I_t = I_o \exp(-\sigma LN) \tag{2.37}$$

where I_t is the transmitted intensity, I_o is the initial intensity, σ is the cross section (cm^2) of the absorbing species at the measured wavelength, L is the path length of the absorbing medium (cm), and N is the number density of absorbing species (cm^{-3}).

When the transmitted intensity and the initial intensity are approximately the same, the absorption is weak and difficult to measure. Also if the light source is a pulsed laser, the pulse-to-pulse variation in the intensity of the laser can mask a weak absorption, making traditional methods insufficient for weak absorption.

In calculating transmittance, T, one uses a ratio of the intensity after passing through the sample to the initial intensity:

$$T = \frac{I}{I_0}. \tag{2.38}$$

A logarithmic relationship exists between absorbance and transmittance:

$$A = -\log T = -\log \frac{I}{I_0}. \tag{2.39}$$

On modern equipment, readout is usually given as transmittance, %-transmittance, or as absorbance.

If the unknown analyte in question is the only absorbing species present in the light beam at a particular wavelength and is present at a sufficient amount, the concentration can be found directly by absorption spectroscopy (AS) using the Beer-Lambert law[3]. A working curve is used to find the concentration if the absorptivity coefficient is unknown. This curve is a plot of the absorption signal at a selected wavelength as a function of the analyte concentration. It is obtained when a series of standards of a known dilution is measured and used to calibrate the linearity of the instrument used.

Several limitations exist in the use of the linearity of Beer-Lambert law:(1) deviation in absorptivity coefficients at high concentrations (>0.01M) due to electrostatic interactions between molecules in close proximity; (2) scattering of light due to particulates in the sample; (3) fluorescence or phosphorescence of the sample; (4) changes in refractive index at high analyte concentration; (5) shifts in chemical equilibria as a function of concentration; (6) non-monochromatic radiation deviations can be minimized by using a relatively flat part of the absorption spectrum, such as the maximum of an absorption band; (7) stray light; and (8) the absorptivity coefficient can be temperature dependent[3].

The Beer-Lambert law is well-established theory, but there are problems with using conventional absorption spectrometric measurements in determining species under

certain situations. The instrumentation may have insufficient sensitivity and a certain lack of specificity in the UV/visible region due to overlapping absorption bands.

In explaining the concepts of emission, at least two energy levels need to be present, E_1 and E_2. Typically E_2 is greater than E_1, with the latter typically being the ground level. When an atom or molecule is the upper level and decays to the lower level, the energy change creates a photon. Also, if the energy is delivered as an electromagnetic wave, spontaneous emission occurs. The corresponding frequency is given as

$$v_0 = \frac{E_2 - E_1}{h}, \tag{2.40}$$

where h is Planck's constant. Decay can also take place in a nonradiative way as well. This event is referred to as ronradiative decay[4]. Returning to our previous scenario where E_2 is greater than E_1, consider the atom under observation in the upper level. Let the frequency of the incident electromagnetic wave be equal to that of the emitted wave, $v=v_0$. With the emitted frequency equal to an atomic transition frequency, a chance of the energy moving from the higher to the lower energy level is still possible. The difference of the energies here is released in the form of the electromagnetic wave in addition to the incident wave. When this happens, it is called stimulated emission.

Spontaneous emission and stimulated emission are not the same. In the former emission process, an atom emits a wave (photon) that has no definite phase relation to the wave (photon) emitted by another atom, and the wave (photon) can be released in any direction. As for stimulated emission, the emission of the atom has to be in phase with the incoming wave and in the same direction. In either case, emission is considered as photon creation.

In explaining the concept of absorption, at least two energy levels must also be present, E_1 and E_2withE_2 greater than E_1[4]. When atoms or molecules go from a lower to a higher temperature, they become excited and can energize the unpaired valence electrons. When enough energy is provided, the valence electrons can jump from a lower level (E_1) to a higher level (E_2)[5]. The very fast transition is called a quantum jump, usually lasting only in the range of nanoseconds or less. The energy difference is generated from the energy of the incident electromagnetic wave. This process is called absorption. Absorption is also called photon annihilation.

In both emission and absorption, a number of atoms or molecules must be involved. The number of atoms or molecules at a given time in level *i* is represented by N_i. N_i is also referred to as the population of a level *i*. To fit the above scenarios, we will let *i* represent levels 1 (ground) and 2 (excited).

Since the number of atoms or molecules is changed in emission and absorption, a rate, $\frac{dN_i}{dt}$, has to be defined. Pertaining to spontaneous emission, the rate from the upper level (2) must be related to the population of the same level. This equation is given by

$$\left(\frac{dN_2}{dt}\right)_{sp} = -AN_2 \tag{2.41}$$

where A is the rate of spontaneous emission or Einstein A coefficient which has units of hertz. The reciprocal of the Einstein coefficient is the spontaneous lifetime, τ_{sp}. The nonradiative decay (n_r) follows the same protocol. There is a difference between spontaneous and nonradiative decays. The lifetime of spontaneous decay depends only on the considered transition; the nonradiative decay depends not only on the considered

transition, but also on the surrounding medium as well. Similarly, stimulated processes of absorption and emission follow the same procedures.

The process of stimulated emission is represented by,

$$\left(\frac{dN_2}{dt}\right)_{st} = -W_{21}N_2 \tag{2.42}$$

where W_{21} is the rate of stimulated emission from a higher energy state (2) to a lower energy state (1) and has the same units as A. The distinction between A and W_{21} is that the later depends not only on transition, but also on the intensity of the electromagnetic wave as well. In terms of absorption,

$$\left(\frac{dN_2}{dt}\right)_{a} = -W_{12}N_1 \tag{2.42}$$

where W_{12} is the rate of absorption from the lower energy state (1) to a higher energy state (2). The two rates (W_{12} and W_{21}) for a plane wave share a common variable known as the flux, F. In stimulated emission,

$$W_{21} = \sigma_{21}F \tag{2.43}$$

where F is the flux mentioned above and σ_{21} is the cross section of the emission which depends on the specific transition. The cross section is written with units of area. The emission's counterpart has a similar relationship with flux also; the equation is given as

$$W_{12} = \sigma_{12}F \tag{2.44}$$

where σ_{12} is the cross section of the absorption. The absorption cross section also depends on the specific transition, and has the same units as the cross section of emission. If the lower energy state is equal to the upper energy state, the two energy rates are equal

(nondegenerate): $W_{12} = W_{21}$. The same applies to the cross sections of emission and absorption: $\sigma_{12}=\sigma_{21}$.

Lasers

The theoretical concept of Light Amplified by Stimulated Emission of Radiation, whose acronym is laser, was originated by Townes and Arthur Schawlow in 1958. In 1960, Theodore H. Maiman made the theory a reality [5].

There are three basic concepts of the workings of a laser: (1) an active medium which strengthens the electromagnetic wave; (2) an energy pump with propels energy into the active medium to populate certain levels to initialize population inversion; (3) an optical resonator which houses part of the induced emission[6].

In a given material, two energy levels (E_1 and E_2) have populations of N_1 and N_2, respectively. Consider a plane wave with a flux in the z direction. A change in flux is generated and labeled *d*F as it travels in the z direction[4]. This change in material is directly related to stimulated absorption and emission processes. The cross section of the beam is an area S. The volume per unit of time is given by S*d*F, which represents a difference in stimulated emission and absorption. A relationship among W_{21} (the rate of stimulated emission), W_{12} (the rated of absorption), N_1 and N_2 (the populations), Sdz (the volume of interest), S*d*F (the volume per unit of time), and z (the change of direction) is given as:

$$SdF = [W_{21}N_2 - W_{21}N_1]Sdz \tag{2.45}$$

Including the relationship of the rates to the surface areas, the previous equation becomes

$$dF = F\sigma_{21}[N_2 - \frac{\sigma_{12}}{\sigma_{21}}N_1]dz. \tag{2.46}$$

If $N_2 > \frac{\sigma_{12}}{\sigma_{21}}$, the material performs as an amplifier; if $N_2 < \frac{\sigma_{12}}{\sigma_{21}}$ the material performs as an absorber[4]. Population inversion occurs when $N_2 > \frac{\sigma_{12}}{\sigma_{21}}$, and the material serves as an active medium. If the transition frequency ν_0 falls in the microwave region, the amplifier is known as a maser (Microwave Amplified by Stimulated Emission Radiation); if it falls in the visible region it is known as a laser (Light Amplified by Stimulated Emission of Radiation).

The overall objective of the pumping scheme of the laser is to induce population inversion[4]. In the two-leveled system discussed earlier, population inversion does not work since the absorption and stimulated emissions counterweigh each other. This is called a two-level saturation since the material becomes transparent (Figure 2.1)

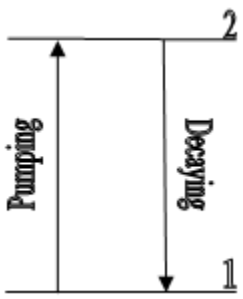

Figure 2.1 Two-level pumping scheme

In a three-level system, level 1 is referred to as the ground level. Atoms or molecules are raised from the ground level (1) to the highest level (3) and quickly decay to level 2. Population inversion occurs between levels 1 and 2

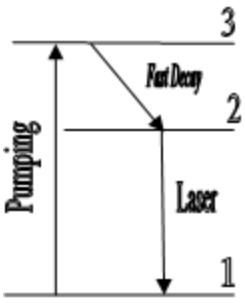

Figure 2.2 Three-level pump scheme

Similar to the three-level system, in a four-level system, atoms or molecules are raised from the lowest level (0) to level 3, quickly decaying to level 2. Population inversion occurs in this system as atoms or molecules transfer from level 2 to level 1. Through stimulated emission, are atoms transferred into level 1. If in a continuous wave (CW) mode, transitions must occur quickly

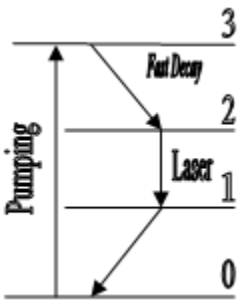

Figure 2.3 Four-level pumping scheme

Comparing the last two levels mentioned, the four-level system has more stability than the three-level system. In the three-level scheme, as the atoms are raised to the highest level and decay to the level 2, the highest level is more or less empty. If level 1 represents a state of equilibrium, if $N_2=N_1$, and if $\sigma_{12}=\sigma_{21}$, the change of flux is zero in Eqn(2.46). In the four-level system, as the atoms are raised to the 2nd highest level (2),

any transition to level 1 induces population inversion since level 1 is empty. These actions are referred to as pumping.

The most commonly used resonators in lasers are mirrors, typically circular in shape. The distance separating them (L, in tens of centimeters) is almost one order of magnitude compared to their diameters[4]. The wavelength of a laser must be shorter than the dimensions of the resonator. The distance between the mirrors, L, is an integral number of half wavelengths apart for stability. If the two were equal, the gain would not allow laser oscillation. Resonators of lasers are open to reduce the number of nodes that can oscillate; if open, the number of nodes increases dramatically. By being open, only a few nodes correspond to the superposition of waves traveling in the direction of the resonator axis. This low loss allows laser oscillation from the reflection of the electromagnetic field. This electric field in a cavity is represented by the equation

$$E(r,t) = E_0 u(x,y,z)\exp[(\frac{t}{2\tau_c} + j\omega t)] \tag{2.47}$$

where j is complex and τ_c is the cavity photon decay time proportional to the square of the magnitude of the electric field.

The mirrors have reflections that are not equal to unity (R=1), generating a loss within the cavity. The intensity of the oscillatory field is proportional to the electromagnetic field. The mirrors used to generate reflections have values of R_1 and R_2. Since the mirrors have reflective values less than unity, a fractional loss per pass, T_i, is present. With intensity being a function of time, the intensity after one round trip is

$$I(t_1) = R_1 R_2 (1 - T_i)^2 I_0 \tag{2.48}$$

where I_0 is the initial intensity[4]. With the value of the length being L, the time after each pass is

$$t_n = \frac{2nL}{c} \tag{2.49}$$

As the intensity is reduced by each pass, the above equation becomes

$$I(t_n) = [R_1 R_2 (1 - T_i)^2]^n I_0 \tag{2.50}$$

The shape of the mode remains the same after each round trip, reinforcing the number of photons in the cavity at a given time, $\phi(t)$, which is proportional to the intensity at that time. The relationship between the number of photons and the intensity is directly proportional and is given as 3

$$\phi(t) = [R_1 R_2 (1 - T_i)^2]^n \phi_0 \tag{2.51}$$

where ϕ_0 is the initial number of photons.

Since the intensity is proportional to the square of the magnitude of the electric field,

$$I = c\varepsilon_0 E^2 \exp(\frac{-t}{\tau_c}). \tag{2.52}$$

Because the photon delay is independent of the number of round trips made,

$$\tau_c = \frac{2L}{c \ln[R_1 R_2 (1 - T_i)^2]} \tag{2.53}$$

The logarithmic denominator of the previous equation is the cavity loss γ.

A plane parallel (Fabry-Perot) resonator has two mirrors that are parallel to each other and longitudinal. The cavity length (L) is an integral of half-wavelengths

$$L = \frac{n\lambda}{2} \qquad .(2.54)$$

and n is a positive integer. Because of this, the electromagnetic wave at the two mirrors cancels. Using the relationship between wavelength, frequency, and the speed of light, the above equation for frequency can be written as

$$\upsilon = \frac{nc}{2L} \qquad (2.55)$$

If the integers differ consecutively (i.e. differ by 1), then the change of frequency becomes

$$\Delta\upsilon = \frac{c}{2L}. \qquad (2.56)$$

This is known as the frequency difference.

A cavity of a confocal resonator consists of two mirrors which are a distance of L apart witha frequency calculated by

$$\upsilon_{mnq} = \left(\frac{c}{2L}\right)\left[q + \frac{1}{2}(m+n+1)\right] \qquad (2.57)$$

where c is the speed of light, qis a large integer, and m and n are small integers[7]. These integers are referred to as transverse modes. Ideally, a laser of mode TEM_{00} is the best since it has the smallest focal spot and highest irradiance. Higher TEM's are distributed and affect the focusing of the laser beam.

Arrhenius Rate

A commonplace correlation was found by a 19th century Swedish chemist by the name of Svante Arrhenius: the rate of reaction increases as the temperature increases. The rate of chemical reaction was found to increase exponentially as the absolute temperature increased. The equation for this rate:

$$Rate = Ae^{xT} \text{ or } Rate = Ae^{-B/T} \tag{2.58}$$

where A and B are empirical and differ for each reaction. B is the amount of energy molecules must have to react. The value B is similar in many reactions, and the rate of reaction doubles in 10°C increments[8].

The kinetics of the reactions is understood by replacing B by E_a/R, where E_a is the activation energy (the energy of the activated relative to the average energy of the reactant molecules) and R is the universal gas constant (8.31J/(gmol·K)). The rate is redefined as

$$Rate = Ae^{-E_a/(RT)} \tag{2.59}$$

The variable A is a pre-exponential factor or frequency factor. The activation energy as well as the frequency factor can be found by using several temperatures for each reaction. A semi-logarithmic plot of the rate against the inverse of the temperature will give a straight line with a slope of E_a/R and an intercept of ln(A). This is referred to as an Arrhenius plot. If the temperature encompasses a wide range, additional terms will be needed. In bimolecular gas-phase reactions, the rate is defined as:

$$Rate = A' T^{1/2} e^{(-E'_a/RT)} \tag{2.60}$$

Complicated expressions are rarely justified by the precision found in experimental data. If large deviations are present, the rate constant is a combination of rate constants for elementary reactions with different values of E_a

The energetic material of this thesis was 2,4,6-trinitrotoluene or TNT for short. Energetic materials (EMs) are environmental health hazards[9]. Soils of many military bases have been infected by EMs which are also nitrogen based. A common nitrogen-based compound is fertilizer. According to the Fertilizer Act, fertilizers are to be listed by weight percentage of nitrogen (N_2), phosphate (P_2O_5), and potash (K_2O). Fertilizers have similar features to low levels of TNT in soil (such as a 400mg sample with 40mg of fertilizer added).

The molecular formula of TNT is $C_7H_5(NO_2)_3$, and its a molecular weight is 227.1g/mole. The melting of this material occurs at only 82°C, but the temperature for auto-ignition is 475°C. There are two densities for TNT: 1.47g/cm^3 (molten) and 1.654g/cm^3 (crystal). The solubility of TNT toluene in water is only 0.01% at 25°C, making it nearly insoluble in water; however, it is somewhat soluble in alcohol and very soluble in benzene, toluene, and acetone.

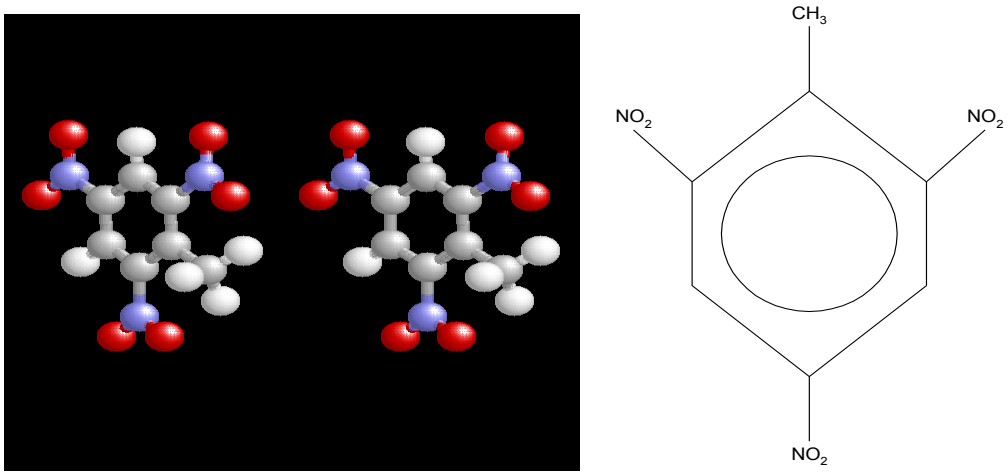

Figure 2.4 Schematic chemical structures of 2,4,6-trinitrotoluene (TNT)

2,4,6-trinitrotoluene is produced by nitration of toluene with a combination of nitric and sulfuric acids. The reaction requires a high concentration of mixed acids that free SO_3. This is a continuous method. There is no other isomer other than 2,4,6 produced by this reaction. The procedure is completed by recrystallization in alcohol and benzene (organic solvents) in 62% nitric acid. Its solidification (melting) can be used as an indication of the purity of TNT. For military grade TNT, the point of solidification is 80.2°C; for pure 2,4,6 TNT, the temperature is 80.8°C. Using nitric acid and recrystallization, solidification (melting) points of 80.6°C and 80.7°C are available.

TNT is the most important explosive for blasting charges[10]. It is very stable and neutral. Casting and pressing are two ways of shaping the charge of the explosive. If pressed, it is cap-sensitive. Care must be taken: the explosive is sensitive and does not require phlegmatizers (wax). Also it is versatile: it can be applied pure, with ammonium nitrate, aluminum powder, RDX (1,3,5-trinitroperhydro-1,3,5-triazine), and other combinations.

Health considerations must also be emphasized as well. This hazard accounts for 20 of 1430 (1.4%) of the National Priorities List[11]of the US Environmental Protection

Agency (EPA), and it is a possible human carcinogen. A compound qualifies as a candidate for the National Priorities List by having such factors as:

1. Having likelihood of having hazardous potential and being released into the environment;
2. Characteristics of toxicity;
3. Affect on people and the environment.

By EPA's standards, these factors can be found in[12]:

1. Ground water migration (drinking water);
2. Surface water migration (drinking water, human food chain, sensitive environments);
3. Soil exposure (resident population, nearby population, sensitive environments);
4. Air migration (population, sensitive environments).

Several factors listed above can be applied to TNT.

The effects of TNT intravenously are anemia, abnormal liver function, skin irritation, and cataracts[13]. This is possible also through the contamination of drinking water.

Many energetic materials infected military bases around the country. These materials are soluble in ground water, making cleanup as well as detection of them difficult. Currently only a few detection methods are available for soil remediation. Ion mobility spectroscopy (IMS) and mass spectroscopy coupled with gas chromatography (GC/MS) have been studied and have proved themselves acceptable[14]. Nevertheless, the drawback with these procedures is the time required for analysis; a sample has to be collected and sent to a laboratory for detection. This time delay can vary from days to

weeks. Another procedure, which has entered the forefront is photofragmentation-laser-induced fluorescence (PF-LIF).

Photofragmentation-Laser-Induced Fluroescence Spectroscopy

Photofragmentation laser-induced fluorescence (PF-LIF) has made drastic improvements in the area of detection. Laser-induced fluorescence (LIF) goes back to 1969 with a group headed by Szkurai and Broida studied LIF spectra of NO_2 [15]. The process of PF-LIF involves the use of a laser to photofragment the material of interest to release a signature material. In the study of TNT by way of photofragmentation laser-induced fluorescence, a laser is set at a particular wavelength and sends out a beam to bombard an energetic material (EM), such as TNT. The signature wavelength of the laser for detection was 226nm, making the energy 5.5eV. When the laser beam hits the TNT, the material breaks down into subcomponents, specifically another molecule and NO_2, the first signature material of interest. Next, NO_2 absorbs an ultraviolet (UV) photon from the laser causing it to predissociate into NO and an oxygen atom. NO, the by-product of interes,t then absorbs a UV photon from the laser and becomes electronically excited.NO* fluoresces and it is the characteristic fluorescence of NO that is detected. In nitro compounds, photofragmentation and predissociation occur at the same UV wavelength.

Photofragmentation occurs in TNT releasing NO_2:

$$C_6H_2CH_3(NO_2)_3 + h\nu \rightarrow C_6H_2CH_3(NO_2)_2 + NO_2\ (X^2A_1) \qquad (2.61)$$

NO_2 absorbs a UV photon, initiating its predissociation to form NO and oxygen atom:

$$NO_2\ (X^2A_1) + h\nu \rightarrow NO\ (X^2\Pi) + O(^1D)/O(^3P) \qquad (2.62)$$

NO absorbs a UV photon and goes into an excited electronic state, causing it to fluoresce:

$$NO\ (X^2\Pi) + h\nu \rightarrow NO(A^2\Sigma^+) \qquad (2.63)$$

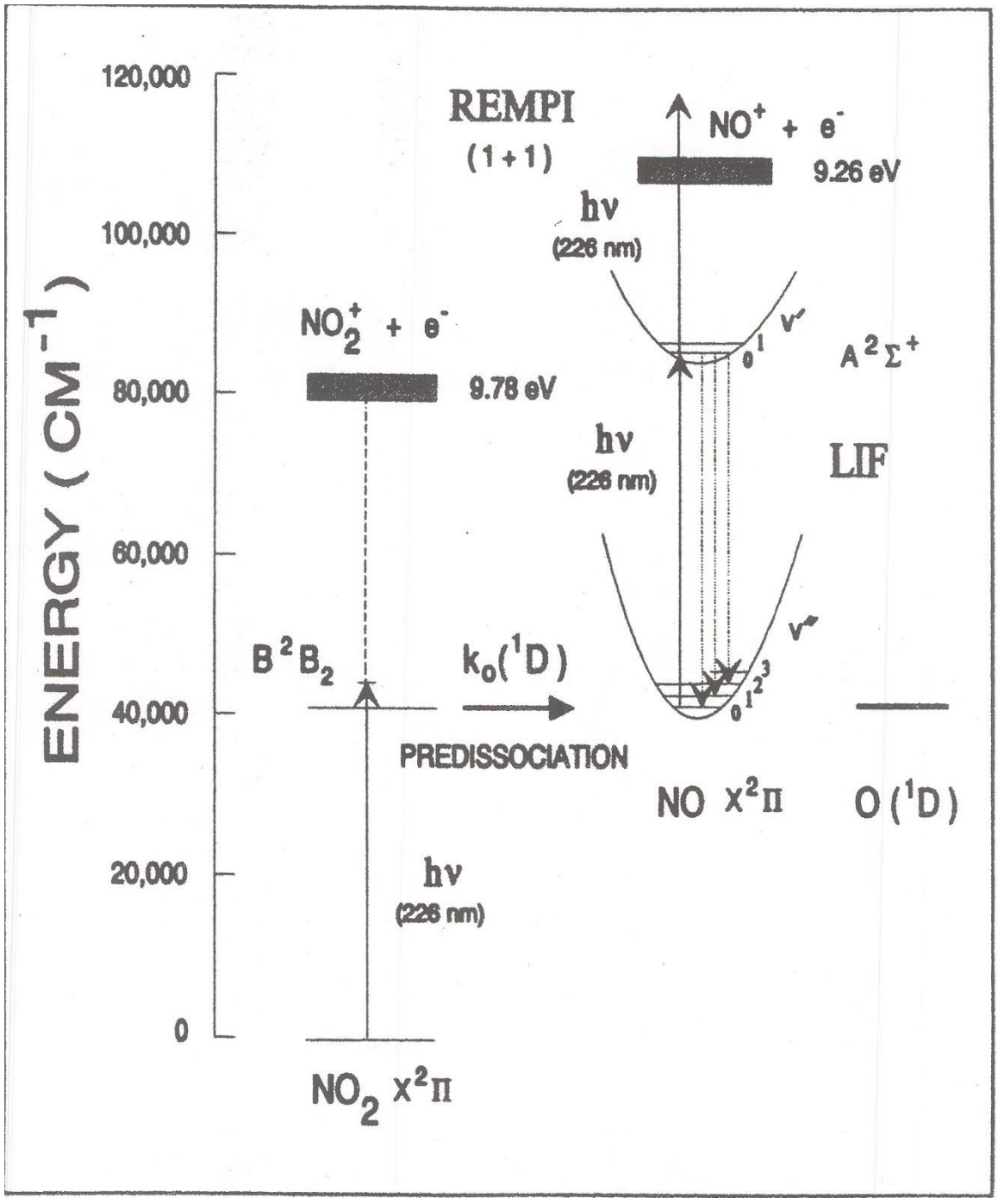

Figure 2.5 Schematic of the photodissociation of NO_2 to form NO, which is then excited into an excited electronic state, leading to fluorescence which is detected as an indicator of photofragmentation.

There are several advantages of using PF-LIF. When analyzing nitro compounds, photofragmentation and predissociation occur at the same wavelength. The concentration of the energetic material of interest is calculated from the intensity of the NO fluorescence. To calculate the concentration of the photons mentioned above,

$$N_{h\upsilon} = \frac{Power_{lightsoure} xtimex\lambda}{hc} \tag{2.64}$$

where λ is the wavelength. No sample preparation is required, and low limits of detection (LOD) have been seen with this technique. Limits of 40 ppb (parts-per-billion) have been reached for TNT[16]. The temperature of the sample studied, the laser power, and the heating time determine the limit of detection of the material under analysis. Photofragmentation occurs according to the Arrhenius equation: the higher the temperature, the higher the rate and thus the greater the photofragmentation efficiency[17]. There is a catch-22 involved here: the cross-section of the EM must be known in advance. The photo-fragmentation cross-section of TNT σ_{PF} (in cm^2) of TNT can be calculated from

$$\sigma_{PF} = \frac{[NO]_{con} xVolume}{[TNT]_{con} xLxN_{h\upsilon}}, cm^2 \tag{2.65}$$

where $[NO]_{con}$ is the concentration produced by photofragmentation of TNT by the light source, $[TNT]_{con}$ is the concentration of TNT in the cell at room temperature T (in degrees Kelvin), $L_{TNT}$is the total length of the cell (optical path length), and $[N]_{hv}$ is the number of photons having frequency ν.

There are several disadvantages of photofragmentation. First it is temperature dependent; the more a sample is heated to higher temperatures, the less intensity is seen after the second examination[17]. If all energetic materials were to abide to this same

breakdown, unless the analyte is readily available, establishing a database of signatures could become problematic. Second photofragmentation detection is also limited by the efficiency of the photomultiplier tube. Finally the excited state of the analyte must have high fluorescence intensity.

Cavity Ringdown Spectroscopy

Cavity Ringdown Spectroscopy (CRDS), also referred to as Cavity Ringdown Laser Absorption Spectroscopy (CRLAS), is a real-time measurement of vapor density of various chemical species, including energetic materials. Its main objective is to measure electronic spectra of molecules and clusters in direct absorption :it can be used to determine absolute vibronic band intensities and access states that are invisible to laser induced fluorescence (LIF) or to resonantly enhanced multiphoton absorption ionization (REMPI) techniques. The advantage of CRDS compared to mass spectroscopy is the mass spectrometry requires significant time up to hours to obtain what CRDS acquires almost instantly[18]. O'Keefe and Deacon introduced the procedure in 1988 by analyzing molecular oxygen in a doubly forbidden transition $b^1\Sigma_g - X^3\Sigma_g$ [19].CRDS can be applied in spectral regions from the ultraviolet (UV) to the infrared (IR). CRDS' application is limited by laser-accessible spectral regions for which mirrors with very high reflectivity can be fabricated. Many molecular transitions are seen better by this procedure than in photoaccoustic spectroscopy. CRDS is considered one of the best measures of absorption spectroscopy. Saykally and coworkers[20]combined CRDS with pulsed vaporization cluster sources to record absorption spectra of Cu_2 and Cu_3 in a supersonic molecular beam [21]. The importance of the Saykally group's experiment was the ability of the procedure to

observe transitions of Cu_3 that were weakly seen in resonant ionization and in LIF experiments due to predissociation of the excited state.

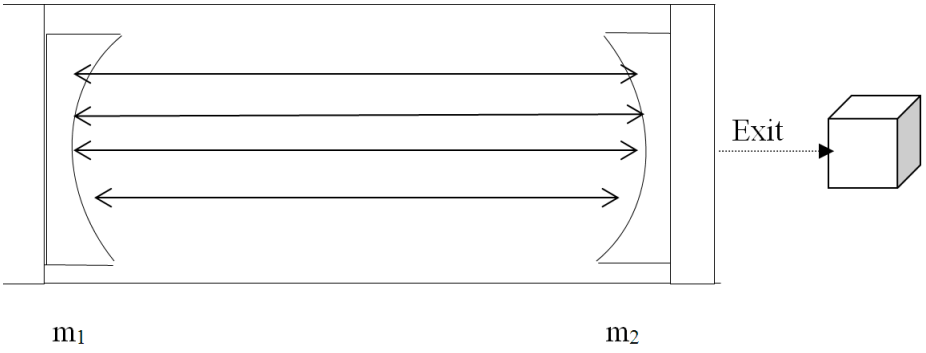

Figure 2.6 Schematic of CRDS apparatus

The CRDS technique uses an optical cavity of two mirrors. These mirrors are concave, dielectric-coated, and required to have very high reflectivities (R>99.9%) (see Fig. 2.6).[21] When light is injected into the cavity, it is reflected back and forth inside. A small fraction is transmitted (approximately 1 minus the reflectivity) through the mirror during each pass. The intensity will decrease gradually with time as energy leaks out of the cavity. The quality of a cavity (Q) is the ratio of energy stored in the cavity to the energy lost by the cavity. The intensity in a cavity with a high quality (Q) will take a longer time to decay than one with a low quality. This intensity of the light between these mirrors decays exponentially at a rate determined by the round trip losses of the pulse. A photomultiplier tube (PMT) placed behind the second mirror is used to monitor the transmitted intensity as a function of time. There is an exponential decay in the intensity with respect to time where the lifetime is defined as the time required to decrease to a value of e^{-1} of that of the original intensity. The technique is called Cavity Ringdown Spectroscopy (CRDS) to indicate that the parameter being measured is the

exponential decay of radiation inside the cavity. A value is calculated by fitting the waveform obtained to a single exponential function. If the spacing of the mirrors is given as d, the equation for calculating the ringdown time, τ, is

$$\tau = \frac{d}{c[(1-R)+\alpha l_s]} \tag{2.66}$$

where d = cavity length, R = reflectivity of mirror, l_s = length of optical path through sample ($d = l_s$ if cavity is gas filled), c =speed of light, and α = absorption coefficient (also written as k(λ) because it is wavelength dependent). As seen in the above equation, the value of τ is a function of mirror reflectivity R, cavity dimensions, and the absorption of sample (α). An inverse relationship exists between the value of the absorption coefficient and the ringdown time, which is a function of the wavelength. With a fixed wavelength (λ), any change that is to occur will derive from changes in the concentration of the analyte under investigation. In the absence of any absorbing species (α=0), the ringdown time is calculated as

$$\tau_0 = \frac{d}{c[(1-R)]} \tag{2.67}$$

The above equations show the importance of the reflectivity of mirrors used in cavity ringdown spectroscopy. If there is a lack of an absorbing species in the volume between the two mirrors, the loss of the cavity occurs from a small transmittance from the mirrors and from losses of typically 0.01% to 0.001% [19]. In essence, most of the energy directed towards the cavity is reflected by the highly polished mirrors of the cavity. If there is an absorbing species present in the cavity that obeys Beer's law inside the cavity, it will cause a loss in the intensity and reduce the quality. This will cause a shorter

exponential decay (ringdown curve) with respect to time than in one where there is no absorbing species present.

In an empty cavity containing two mirrors of the same reflectivity, the intensity inside the cavity will decrease exponentially based on the equation:

$$I(t) = I_o \exp\left[-(1-R)\frac{tc}{L}\right] \tag{2.68}$$

where I(t) is the intensity after time t,I_0 is the intensity at the beginning of the pulse, R is the reflectivity of the mirrors (where R+T=1 in Kirchhoff's law and T is the transmission, also, (1-R) is the loss per reflection), and L is the length of the cavity. The value $\frac{tc}{L}$ is twice the number of round trips after time t (if a cavity has two mirrors, there are two reflections per round trip). Typically, the diameters of the mirrors greatly exceed the beam diameter injected. The decay constant (τ) is half the transit time of a round trip divided by the loss per reflection:

$$\tau = \frac{t_r}{2(1-R)} \tag{2.69}$$

In theory, the cavity usually contains a species that absorbs the wavelength of radiation injected into the cavity. The loss based on absorption is a function of the absorption coefficient according to Beer's law. It is calculated as

$$loss_{ab} = (2\alpha L)\left(\frac{tc}{2L}\right) \tag{2.70}$$

where α is the absorption coefficient calculated from the product of the absorption cross-section and the number density of the absorbing species $(\alpha = \alpha(cm^{-1}) = \sigma N)$. The total loss inside the cavity with an absorbing species is:

$$loss_{total} = (1-R)\frac{tc}{L} + (\alpha L)\frac{tc}{L} = \frac{tc}{L}\left[(1-R)+\alpha L\right] \tag{2.71}$$

Based on this, the equations for the intensity and for the decay constant are rewritten:

$$I(t) = I_0 \exp\left\{-\left[(1-R)+\alpha L\right]\frac{tc}{L}\right\} \tag{2.72}$$

and

$$\tau = \frac{t_r}{2\left[(1-R)+\alpha L\right]} \tag{2.73}$$

When an absorbing species is present in the cavity, the time constant for the ringdown curve is reduced. A graph of the cavity loss versus the wavelength can also give the absorption spectrum.

Combining the two equations pertaining to the decay constant gives another equation for finding the absorption coefficient for the particular species being observed:

$$\alpha = \frac{1}{c}\left(\frac{1}{\tau_1} - \frac{1}{\tau_2}\right) \tag{2.74}$$

where τ_1 is the ringdown time of the cavity containing the absorbing species and τ_2 is the ringdown time of the empty cavity. This value can only be calculated if both ringdown times are known for a particular wavelength.

CRDS has several advantages over PF-LIF. CRDS can collect data in real time and works at standard room temperature and pressure (STP). The measurement of the decay rate eliminates shot-to-shot variations[18]. With available mirrors, most wavelengths are applicable. The overall setup is compact and relatively inexpensive. The limit of detection is smaller than 1ppb for TNT.

CRDS also has disadvantages. The expensive of the mirrors used is a function of the reflectivity. The reflectivity has to remain constant. Mirrors have a limited spectral

range (typically approximately 50nm). An important factor also is the re-alignment of the setup after each data collection. Since the setup requires the use of two mirrors, the reflectivity of each mirror should be the same. Also, just as with PF-LIF, the concentration of NO can be calculated.

CHAPTER III

OPTICAL PROPERTIES OF GASEOUS TNT IN THE ULTRAVIOLET REGION:

Absorption Spectrum of Gaseous TNT

Absorption spectroscopy (AS) was combined with Cavity Ringdown Spectroscopy (CRDS) in order to determine the absorption cross section of TNT. Two regions of interest were studied. The first region was 195-300 nm using broadband absorption spectroscopy and the second was 225-235nm using CRDS. The TNT absorbance coefficient has a temperature dependence. My study was CRDS study at a wavelength of 230nm in the temperature range of 5-110ºC. After normalization of the collected spectra for both techniques, the cross section of TNT were computed.

In the absorption spectroscopy technique, a xenon arc lamp (Oriel, Model 6254) was used as a 100 W ultraviolet light source with continuous emission (see Fig. 2.1). The sample cell was made of stainless steel components (MDC Corporation) with a length of 52.6cm and a radius 3.5cm. The two ends of the sample cell were closed by UV-grade quartz viewports (Cermaseal). The weight of the TNT sample was 0.3g. TNT was absorbed in 2mL of acetone for the purpose of depositing a coating of TNT inside the cell by swabbing the cell towards the center. After application, the cell was pumped out and filled with argon to 1 atmosphere. Two heating tapes (Thermolyne) were used towards the center of the cell for an even temperature distribution. The temperature regulation of the tapes was done by an autotransformer (Powernet 3PN1010B) with an accuracy of ±0.1ºC as determined by a thermocouple. The second tape heated the viewports which

were 10ºC above the cell's temperature to avoid condensation. The calculation of the partial pressure was done from an equation between temperature and pressure defined by Dionne et al.[22]:

$$\log_{10} P(ppb) = \frac{-5481}{T(K)} + 19.37 \tag{3.1}$$

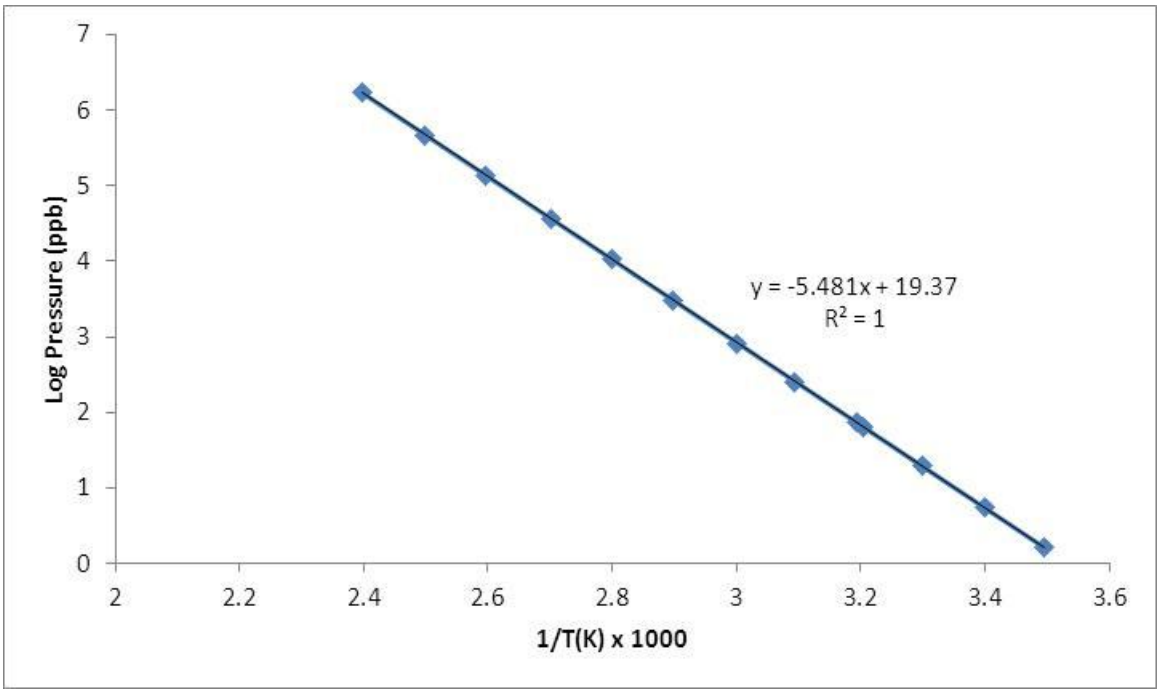

Figure 3.1 Vapor pressure of TNT as a function of inverse temperature calculated from the Dionne equation (2.1)

Absorption spectroscopy data were recorded using a xenon arc lamp operated at 100W; a SPEX spectrometer with a focal length of 1m and a 1800 grooves/mm grating; a solar blind photomultiplier tube (Hamamatsu R166UH); and a digital oscilloscope (Tektronix TDC 410A). A diffuser was used to reduce the dark count of the solar blind photomultiplier tube (PMT). Wavelength calibration of the spectrometer was performed to an accuracy of ±0.005nm using a mercury lamp. Eleven overlapping regions in the

195-300nm spectral range were investigated. Two spectrometer slit widths were used for the collection of the spectra: for the 195-200nm region, the width was 700μm; for the 270-300nm region, the width was 35μm. Spectral resolution was 0.4nm for 195-200nm and 0.02nm for the 270-300nm region. By application of the Beer-Lambert law, the value of the absorption coefficient can be determined:

$$k(\lambda) = \frac{1}{l} \ln \frac{I_o}{I_t} \tag{3.2}$$

where l is the absorption sample length (52.6cm), I_0 is the initial intensity introduced into the cell, and I_t is the transmitted intensity through the cell. Normalizing using the number density, and using Eqn 2.2, the absorption coefficient was found using:

$$\sigma(\lambda) = \frac{k(\lambda)}{N} \tag{3.3}$$

where σ(λ) is the wavelength-dependent cross section which has units of cm^2. A solid TNT sample was used to avoid change of the number density, N, during photofragmentation by a UV light source. From this study the partial pressure of TNT equaled the saturated pressure from (Eqn 3.1). After recording each set of data, the sample cell was cooled.

The CRDS experimental setup used the third harmonic (355nm) of a 10Hz repetition neodymium yttrium aluminum garnet Nd:YAG laser (Continuum NY82S-10) (Fig. 2.3). The duration of the laser's pulse was 7-8 ns. A dye laser (Continuum ND60) used with Coumarin 450 laser dye generated 5 mJ pulses within the spectral range of 445-485 nm. The distance was 454mm between the dye laser and the first lens (focal length 200mm) of the 1X telescope. The telescope contained an iris for proper alignment to the first right-angle prism. Another iris was placed between the first and second

turning prisms, which rotated the laser beam 180° from its original direction. An Autotracker frequency doubling system (INRAD AT-II) with a four-prism wavelength separator filter (INRAD 752-104) doubled the 460 nm wavelength from the dye laser to 230 nm. A 5X telescope composed of 20 mm and 100 mm focal length quartz lenses with an iris of 10 μm between them was used for proper beam alignment. From the second telescope, the ringdown system was approached. The ringdown cavity was composed of two concave mirrors (MLD Technologies), each with a radius of curvature of 6 m. Maximum reflection (99.6%) of each mirror was at 230 nm. Reflectivity was reduced to 99.1% with detuning of ±2.5 nm. Detuning of the mirrors confined the ability to measure the absorption of the TNT sample via the cavity ringdown technique. The decaying spectra were collected with a photomultiplier tube (Hamamatsu R166UH). An iris and a lens were placed in front of the PMT to avoid saturation. The signal from the photomultiplier tube was digitized and collected by a Tektronix oscilloscope (TDS 410A) which was triggered by a GPIB interface and sent to the data acquisition computer.

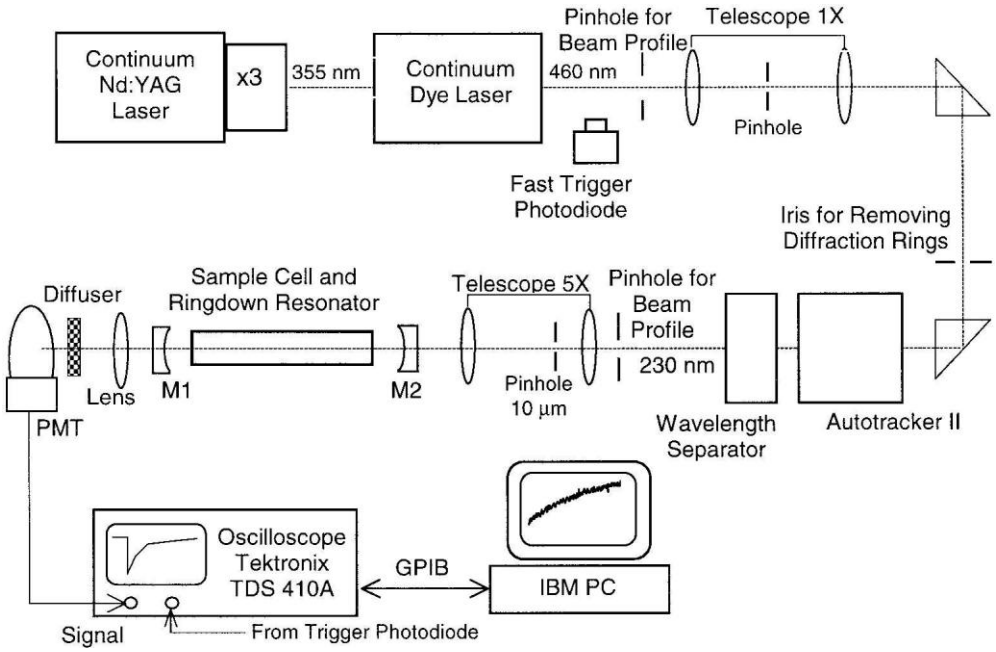

Figure 3.2 Schematic of CRDS apparatus for determining absorption cross section of TNT at 230 nm in the temperature range of 5 to 110°C

By using Eqn (2.66) and Eqn (2.67), the wavelength-dependent absorption coefficient was found by using:

$$k(\lambda) = \frac{L}{cl}\left(\frac{1}{\tau(\lambda)} - \frac{1}{\tau_0(\lambda)}\right) \tag{3.4}$$

where τ_0 is the decay time of an empty cell, τ is the decay time of the occupied cell, and c is the speed of light.

In the latter part of the CRDS experiment, a different cell was used. This cell had a total length (L) of 775mm from mirror to mirror (see Fig 3.3). The mirror reflectivity was 0.996 at 230 nm and the reflectivity was reduced to 0.991 when the wavelength was detuned ±2.5nm. The length (l) of the sample cell was 284 mm. Optical entrance to and exit from the cell is by way of holes of 4 mm diameter and length of 40 mm. The holes replace the viewports previously used in the broadband absorption spectroscopy portion of the experiment. These holes prevented light loss from the cell. The cavity ringdown

part of the experiment was performed to compare with the results of those of the absorption spectroscopy portion. A heating tape (Thermolyne HT) evenly covered the stainless steel cell with a uniform distribution of heat applied. Two thermocouples measured the temperature of the cell to an accuracy of ±0.1ºC. The sample was applied by also by a brush wetted by a TNT and acetone solution.

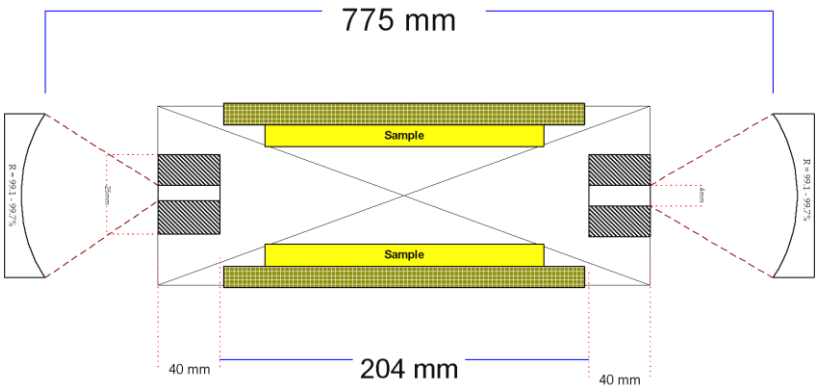

Figure 3.3 Schematic of CRDS cavity and sample cell for TNT measurements

The nitro group absorption by the n→π* electronic transition occurs in the ultraviolet. In an ethanol solution (absorption curve B), absorption of TNT is weaker and shifted to longer wavelengths as seen in Fig 3.5. Peaks in the figure (205nm, 215nm, and 226nm) correspond to NO vibronic absorption [$A^2\Sigma^+(v'=0,1,2) \leftarrow X^2\Pi\ (v''=0)$] transitions and are due to the photofragmentation of TNT, releasing NO molecules. Absorption curve A shows work from this experiment; Line B shows work from Schroeder et al

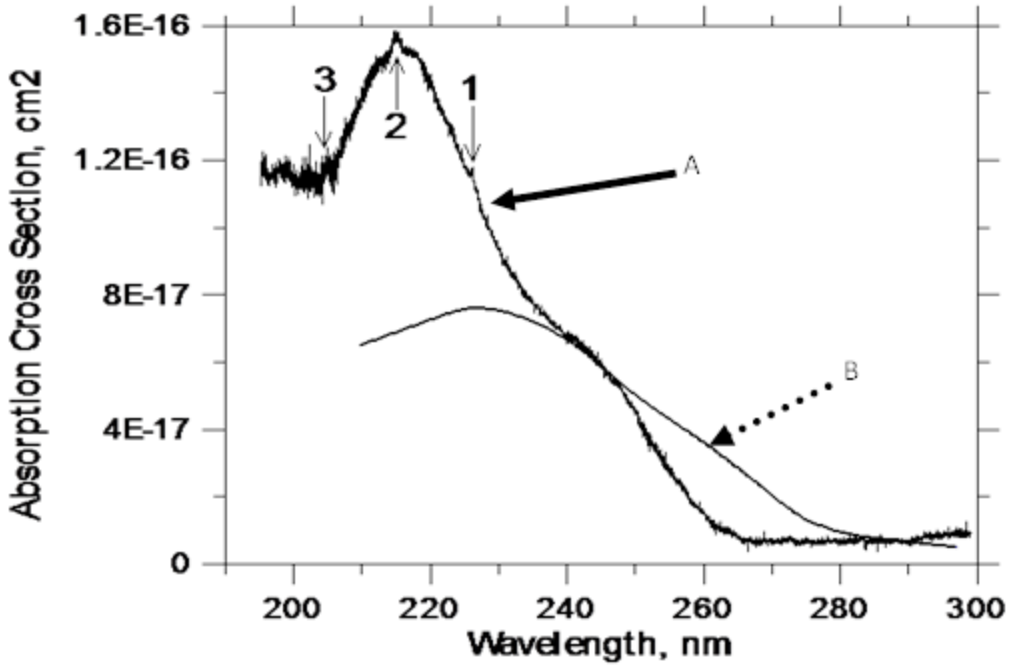

Figure 3.4 Absorption versus wavelength

The solid line (A) represents the gaseous phase of TNT at 92°C. The dotted line (B) represents TNT in an ethanol solution from a reference work[23]. On the solid line, arrows 1,2,3 indicate peaks of absorption of from a ground state to excited state: NO $A^2\Sigma^+(v=0,1,2) \leftarrow X^2\Pi(v=0)$.

With the absorption peaks remaining the same, no significant change was observed in the absorption of TNT after each data set was collected when the cell was cooled to room temperature. Using CRDS, no structure was found in the 225-235 nm region in the vacuum cell with 2 mPa pressure with a spectral resolution of 0.3 cm^{-1}.

Data sets were collected by both techniques in a temperature range of 5-110°C at a wavelength of 230 nm to determine the measured absorption coefficient $k_m(T)$ of TNT in the vapor phase. With λ=230nm, the temperature-dependent absorption coefficient $k_c(T)$, was calculated using Eqns 3.1 and 3.3 when the cross section is 9.4 $x10^{-17}$ cm^2 (extracted from Fig 2.5). Both agreed in the region of 40-50°C. Below and above the region of 40-50°C, values differed:

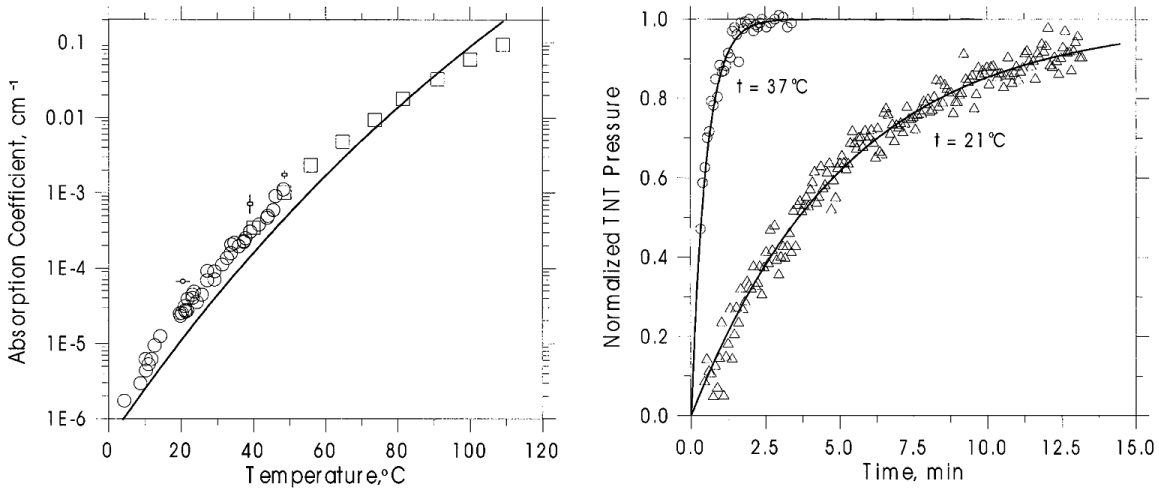

Figure 3.5 Cavity ringdown versus absorption spectroscopy.

A.) The graph on the left shows the temperature dependence of the absorption coefficient of saturated TNT vapor at 230 nm by broadband absorption spectroscopy (squares □) and CRDS (circles ○). The solid curve is the calculated temperature dependence of the absorption coefficient. The small circle with the horizontal bar shows the error of the temperature measurements using CRDS. The two small squares with bars indicate the errors of the absorption coefficient measurement using broadband absorption spectroscopy at 40 and 48.5°C. All other errors are negligible. B.) Real-time measurements of TNT vapor density in cell. At time t=0, the argon flow was stopped. Triangles Δ are the normalized instantaneous TNT vapor density at 21°C while squares□ are the normalized instantaneous TNT vapor density at 37°C

Care should be taken: $k_c(T)$, the calculated temperature dependence, is based on of the cross section at a particular wavelength the for normalization temperature.

There are differences in the temperature at the ends of the temperature range investigated. Equations of the form similar to Eqn 3.1 have been used to approximate temperature dependences of the partial pressure. Eqn 3.1 was a compilation of data collected from seven other findings in the 13-144°C range. No accuracy is given and the curve fit possibly derived from data from experiment of the same temperature range. Another discrepancy in this is setting the two pressures equal ($p_s=p_s(T)$) in the data pertaining to the two temperature dependent absorption coefficients. Experimental and calculated partial pressures are not equal in the 13-30°C and 120-144°C ranges.

Eqn 3.1 is based on the Clausius-Clapeyron equation where the range of temperature is not to be considered. This equation is valid for small changes of temperature. An equation with a wider temperature range and a better approximation is of the form:

$$\log_{10} p_s = \frac{A}{T} + B + C\ln(T) \tag{3.5}$$

From this equation, the absorbance cross section from Eqn (3.4) in the 195 – 300 nm can have a discrepancy of 10% rather that 50% as from Eqn 3.1. Noise of only 0.5-10% determines the relative error a spectral region.

In Figure 3.6b, the vapor densities are real-time measurements taken at temperatures of 21°C and 37°C after purging the cell with argon. Data measurements were taken using

$$p_N(t) = 1 - \exp(\frac{-t}{\tau}) \tag{3.6}$$

where p_N is the normalized pressure and τ is the time constant of the TNT evaporation process. The normalized pressure is calculated by the ratio of the instantaneous pressure (p) to the saturated pressure (p_s):

$$p_N = \frac{p}{p_s} \tag{3.7}$$

As Fig 3.6b shows, TNT measurements using cavity ringdown can also be performed at room temperature. In the same figure, the evaporation of TNT at 37°C (τ=0.5 min) occurred a factor of 10 times faster than evaporation at 21°C (τ=5.2 min). From the graph, rates of evaporation were 7 x 10^8 molecules/cm^2 at 21°C and 4 x 10^{10} molecules/cm^2 at 37°C.

Several aspects were considered for the improvement of the limit of detection (LOD) for the cavity ringdown technique. The major limitations of cavity ringdown spectroscopy are reflectivity and determination of the ringdown time. If the signal-to-noise ratio is unity (S/N=1), then the minimum absorption coefficient calculated using reflectivity and loss per path:

$$k_{\min} l = (1 - R)\frac{\delta\tau}{\tau} \tag{3.8}$$

In our experiment R = 0.996 at 230 nm and the uncertainty $\delta\tau/\tau$ was 3-4 % per pass. Curve fitting 25 decay waveforms leads to an uncertainty of only 0.7%. For a cell of 58.7 cm length and the factors listed above, the minimum absorption coefficient detectable by my CRDS apparatus is 2 x 10^{-6} cm^{-1}. From this approximation, a number density of TNT is 2 x 10^{10} cm^{-3} is obtained from Eqn (3.3). This estimate puts the level of detection (LOD) as parts-per-billion (ppb). Work done by Simeonsson, Lemire, and Sausa[24] found LODs of 0.21ppm (parts per million) at 193nm and 1.7ppm at 226nm. Limits of detection could be decreased to the parts-per-trillion (ppt) level if the cell's length were extended from 24 cm to 2-3 m and using mirrors with reflections greater than 99.9%.

CHAPTER IV

PHOTOFRAGMENTATION CROSS SECTION OF GASEOUS TNT AT DIFFERENT WAVELENGTHS

In the last phase of the experiments, the photofragmentation cross section of TNT at room temperature was determined by using CRDS to measure the concentration of NO produced by the wavelength-dependent photofragmentation of TNT and the subsequent photofragmentation of NO_2. The photofragmentation of TNT was produced by light from a xenon arc lamp. Four wavelength-selection filters of different wavelengths were chosen: 254 nm, 300 nm, 340 nm, and 400 nm. Each filter had a bandwidth of 20 nm.

For comparative studies, the setup for this stage of TNT analysis was similar to that described previously in Chapter 3 (see Fig 3.1). For this phase of the experiment a 100 Watt xenon arc lamp was used. The cell was allowed to cool down after each experiment. Data were continuously collected. Exposure times of each run are listed below in Table 1. The same amount of sample and solvent were used: 0.3 g dissolved in 2 mL of acetone. Rather than heating as before (92°C), the cell was at room temperature (30ºC). Only the windows were kept 10ºC above the temperature of the rest of the sample cell to avoid condensation just as before. Also, the pressure was held to 1 atmosphere (760 torr).

Calculation of the photofragmentation cross section of TNT involved several steps starting with photofragmentation:

1.TNT photofragments, releasing NO_2:

$$C_6H_2CH_3(NO_2)_3 + h\nu_{(Xenon\ arc\ lamp)} \rightarrow C_6H_2CH_3(NO_2)_2 + NO_2\ (X^2A_l) \quad (4.1)$$

2. NO_2 absorbs a UV photon, starting predissociation to form NO and an oxygen atom:

$$NO_2\ (X^2A_1) + h\nu_{(Xenon\ arc\ lamp)} \rightarrow NO\ (X^2\Pi) + O(^1D)/O(^3P). \quad (4.2)$$

3. NO absorbs a UV photon and goes into an excited electronic state, causing it to fluoresce:

$$NO\ (X^2\Pi) + h\nu_{(dye\ laser)} \rightarrow NO(A^2\Sigma^+) \rightarrow NO(X^2\Pi) + h\nu_{(fluoresce)} \quad (4.3)$$

4. Detection of the NO signature was identified by absorption using cavity ringdown:

$$NO\ (X^2\Pi) + h\nu_{(dye\ laser)} \rightarrow NO(A^2\Sigma^+) \quad (4.4)$$

The cell length (L_{TNT}) was 52.6cm and the stainless steel cell had a volume (Volume) of 851.4 cm^3. The power of the lamp was based on the wavelength of the filter used. The calculation of the energy was:

$$E_t = Pxt\ . \quad (4.5)$$

The number of photons $[N]_{h\nu}$ was wavelength-dependent:

$$[N]_{h\upsilon} = \frac{Pxtx\lambda}{hc} \quad (4.6)$$

$$[TNT]_{con} = \frac{p}{kT(K)} \quad (4.7)$$

where k is the Boltzmann constant ($1.38x10^{-23}$J/K) and T is room temperature. From Eqns 3.1, 3.2, 3.2, the cross section of TNT was calculated:

$$\sigma_{TNT-NO} = \frac{[NO]_{con} x Volume}{[TNT]_{con} x L_{TNT} x [N]_{h\nu}} \text{ , cm2} \quad (4.8)$$

The table below gives numeric values from the above equations.

Table 4.1 Photofragmentation and absorption cross sections parameters

Filter (nm)	Power (mW)	Exposure time (min)	E_t (J)	$[N]_{NO}=\alpha/\sigma$ (per cm^3)	N (TNT) (per cm^3)	$[N]_{h\upsilon}$
254	0.1	154	10.80	2.5E12	6.2E11	1.18E18
300	0.115	145	12.08	2.25E12	6.2E11	1.51E18
340	0.38	168	22.68	1.6E12	6.2E11	6.56E18
400	0.75	332	78.44	3.75E12	6.2E11	3.01E19

Table 4.2 Photofragmentation and absorption cross sections as a function of wavelength

Wavelength (nm)	σ_{TNT-NO} at RT[1] (cm^2/molecule)	σ_{NO2-NO} at 21 °C [2] (cm^2 /molecule)	σ_{PF-TNT} at RT[1] (cm^2 /molecule)	σ_{Ab-TNT} at 92 °C [3] (cm^2 /molecule)
254	4.84E-17	1.05E-20	4.839E-17	4.E-17
300	3.41E-17	1.32E-19	3.397E-17	1.E-17
340	5.58E-18	4.02E-19	5.178E-18	
400	2.85E-18	6.44E-19	2.206E-18	

[1] This work.
[2] $NO_2+h\nu \rightarrow NO + O$: Data from Chemical Kinetics and Photochemical Data for Use in Atm. Stud., Eval. No. 15, Sec. 4
[3] TNT absorption cross section at 92 °C reported Appl. Spectrosc. 55 (2001) 125.

The cross sections of this phase of the experiment at room temperature are greatly improved compared with obtained earlier at 92°C (9.4×10^{-17} cm^2). The cross section of TNT is inversely proportional to the wavelength. If extrapolated, a significant improvement could occur in the 220 – 230nm region.

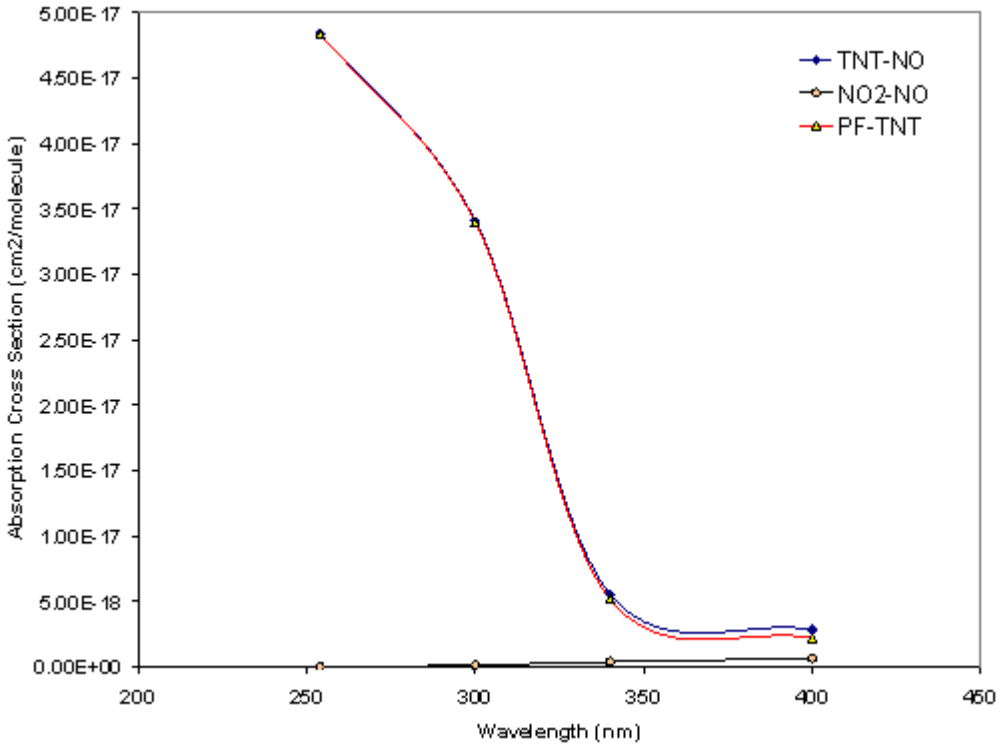

Figure 4.1 Photodissociation cross section (in cm^2) of TNT as a function of wavelength

As mentioned before, a shortcoming of the PF-LIF technique is the necessary knowledge of the cross section at the particular wavelength investigated. In this stage of the analysis, photofragmentation must occur at the wavelength investigated using the combination of laser and lamp through the filter used. The filters chosen must permit the photofragmentation breakdown of the sample.

CHAPTER V

SUMMARY AND CONCLUSIONS

In my thesis I have done work on finding the cross section of TNT in the ultraviolet region using three procedures: 1. broadband absorption spectroscopy; 2. cavity ringdown spectroscopy; and 3. a combination of absorption and cavity ringdown spectroscopy.

Chapter Two of my thesis covered the use of broadband absorption spectroscopy. A xenon arc lamp perpendicular to the sample cell used was used to measure absorption cross section TNT. The sample was heated to 92°C during each run of data collection.

Chapter Two of my thesis also covered the use of cavity ringdown spectroscopy. In an attempt for accuracy, Chapter Three covered the use of absorption spectroscopy on a TNT sample. Chapter Four combined procedures to determine the photofragmentation cross section of TNT as a function of wavelength. Four filters were used (254 nm, 300 nm, 340 nm, and 400nm).

In each method of detection, the cross section was found to be inversely proportional to the wavelength. Identical mirrors with a reflectivity of 99.6% were used in each part. Accuracies of detections are shown in Tables 4.1 and 4.2.

Further work can be done on this and other energetic materials (EMs) using these procedures as well as others. The detection of EMs can be addressed better using cavity ringdown at STP (standard temperature and pressure) as well as vapor phase analysis. Also databases can be established with procedures done in my thesis.

REFERENCES

1. Herzberg, Gerhand The Spectra and Structures of Simple Free Radicals The Spectra and Structures of Simple Free Radicals, An Introduction of Molecular Spectroscopy, Dover Publications (1971).

2. Hollas, J. Michael, Modern Spectroscopy 4 th Edition, John W iley and Sons, Ltd. (2004) , Pg. 154

3. ("Beer-Lambert Law" http://elchem.kaist.ac.kr/vt/chem-ed/spec/beerslaw.htm, Tissue, B.M., 1996.) Pg. 15:

4. Svelto, Orazio, Principles of Lasers, 4th Edition, Springer (1998) Pg. 2

5. Pg 16: Hecht, Eugene, Optics,4th Edition, Pearson Addison (2002), pg 64)

6. Demtroder, W., Laser Spectroscopy: Ba sic concepts and Instrum entation, 3rd Edition, Springer, (2003) pg.221

7. Singh, Jagdish, Thakur, Surya N. Laser-Indu ced Breakdown Spectroscopy, Elsevier, (2007) Pg.5)

8. Umland, Bellama General Chemistry, 3rd Edition, Brooks Cole Publishing, (1999) Pgs. 712-713)

9. Canter, L.W., Nitrates in Groundwater, CRC Press, (1996)

10. Yinon, Jehuda, Zitrin, Shmuel, Modern Methods and Applications in Analysis of Explosives, Wiley, (1993) Pgs 2-5

11. "Toxicological Profile of 2,4,6-Trin itrotoluene" http://www.astdr.cdc.gov/ toxprofiles/tp81.pdf

12. "Introduction to the HRS (Hazard Ra nking System)", http://www.epa.gov/ superfund/programs/npl_hrs/hrsint.htm

13. "Agency for Toxic Substances and Disease Registry ToxFAQs, Septem ber 1996", http://www.atsdr.cdc.gov/toxfaqs/tfacts81.pdf, Pgs.1-2, (Pg 30)

14. Eck, D.L., Kurth, M.J., and Macmillan, C., Immunochemical Methods for Environmental Analysis, ACS Symposium Series 442, American Chemical Society, Washington, D.C., 1990, Chapter 9 (pgs. 79-94)

15. K. Sakurai and H.P. Broida, J. Chem. Phys. 50, 2404-2411 (1969)

16. Boudreaux, Gary M., "Development of A Photoframentation-Laser Induced Fluorescence (PF-LIF) Laser Sensor For Detection Of 2,4,6-Trinitrotoluene (TNT) in Soil and Groundwater" M.S. in Physics thesis, Mississippi State University,(1997)

17. Wu, Dongdong, "Detection of 2,4,6-Trinitrotoluene by Photofragmentation-Laser Induced Fluorescence (PF-LIF) Spectroscopy", M.S. thesis, Mississippi State University, (1996)

18. Cavity Ring-Down Spectroscopy, Wheeler, Newman, Orr-Ewing, Ashfold, pgs 337-351 Journal of Chemical Society Vol. 34, 1988,Pg 337-351.

19. "Cavity Ring-down optical spectrometer for absorption measurements using pulsed laser sources", O'Keefe, Anthony, Deacon, A. G. David, Rev. Sci. Instrum. 59 (12), 1988

20. A. O'Keefe, J.J. Scherer, A.L. Cooksy, R. Sheeks, J. Heath and R.J. Saykally, Chem. Phys. Lett., 1990, 172, 214

21. "Cavity Ringdown Laser Absorption Spectroscopy", Analytical Chemistry News & Features, May 1, 1997 Pg 25-51

22. "Vapor Pressures of Explosives", Dionne, B.C., Rounbehler, Achter, E.K., Hobbs, J.R., Fine, D.H., Journal Applied Spectroscopy Journal of Energetic Materials Vol.4, 447-472, 1986.

23. "Ultraviolet and Visible Absorption Spectra in Ethyl Alcohol", Schroeder, W.A., Wilcox, P., Trueblood, A.O., Analytical Chemistry, Vol. 23, Pgs. 1740-1747, 1951.

24. Applied Spectroscopy, 47, 1993

25. Usachev, A.D., Miller, T., Singh, J.P., Yueh, F., Jang, P., Monts, D., "Optical Properties of Gaseous 2-4-6-Trinitrotoluene in the Ultraviolet Region", Applied Spectroscopy 55, 125-129, 2001